2014 IEEE International Conference on Robotics & Automation (ICRA)
Hong Kong Convention and Exhibition Center
May 31 - June 7, 2014. Hong Kong, China

Passive Stability of a Single Actuator Micro Aerial Vehicle

Matthew Piccoli[1] and Mark Yim[2]

Abstract— **In this work, we present a low-cost, flying research MAV, comparable to common quadcopter platforms. We propose a flyer with only two moving parts (a rotor and a stator) and a single actuator that is capable of hovering flight without active attitude control. The passive stability is analyzed and reduced to two mechanisms that are a function of the relative offset of the center of pressure and center of mass, the angular momentum of rotor and stator and the differential lift of the spinning elements. The design space over these parameters is explored with a dozen models that are unstable and one that is stable. Interestingly, the two stability mechanisms are not compatible requiring opposing design emphasis. Passive stability of this model is verified by Routh Hurwitz criterion, in simulation and a physical prototype. The vehicle has the added benefits of low complexity and favorable size scaling compared to other MAVs. The vehicle design guidelines derived from both theory and experimentation are presented.**

I. INTRODUCTION

In the last two decades, there has been an increased interest in micro air vehicles (MAVs), particularly for surveillance and reconnaissance, the exploration of hazardous or unreachable locations, and the transportation and delivery of payloads. With the advent of higher density batteries, more efficient motors, and light-weight, high-strength materials, MAVs have become more feasible.

These robotic air vehicles can hover and be arbitrarily positioned in 3D space. Lowering the cost of MAVs to be a commodity product would allow large numbers to be feasible and enable a new class of application. Large scale distributed sensing could be used to aid in applications such as forestry, airport or shopping mall security. Being low cost enables uses that would not be otherwise considered. Individually, low cost and simple MAVs would also democratize the use of these devices and fit many consumer applications including robotic information aids and personal assistants. Toys are the initial growing market of these types of vehicles.

Thus the design goals of this work are foremost to minimize cost and size for a flying device capable of holding an arbitrary position in space. A key characteristic of this flying device is passive stability. While many MAVs employ active stability, passive stability will not only be more robust, but will lower the cost of the control electronics.

A. Previous work

MAVs come in many forms, each with their own pros and cons. The most common is the conventional helicopter configuration. This includes one main rotor, controlled with a swashplate, and a vertical tailrotor, which requires two DC motors and three servos. This is the most common platform for groups that are not interested in designing their own flyer, and instead purchase a hobby device. They have been used as scaling testbeds [1], camera tracking testbeds [2], flight control system platforms [3] [4] [5], and autonomous acrobatic helicopter platforms [6], [7], [8].

Also common are coaxial helicopters. These include two large horizontal rotors, axially aligned. Some also have a third small horizontal tail for pitching. They are less maneuverable than conventional helicopters, but are simpler in construction and more compact. Although common among low end hobby flyers, researchers tend to design their own coaxial helicopters for the purpose of aircraft material research [9] and scaling of rotorcraft [10], [11].

Quadrotors have been increasing in popularity with the recent improvement in microelectromechanical systems (MEMS) gyroscopes and accelerometers. Unlike conventional and coaxial helicopters quadrotors are typically actively stabilized, thus requiring sensors like MEMS gyroscopes and accelerometers. The complex controls are countered by a very simple mechanical design. By definition, quadrotors have four continuous rotation motors with horizontal propellers aligned symmetrically and equidistant from the center of mass. Quadrotors tend to be slightly less efficient due to the reduced size of each propeller for a given sized flyer. Although commonly operated around hover, recently there has been an increased interest in aggressive maneuvers [12], [13]. Other areas of research are multi-agent control testbeds [14], [15], stability control testbeds [16], [17], [18], and design [19], [20].

Since this paper aims to address simple and low cost flying devices, it is reasonable to consider devices available as toys. The simplest related flying device may be what has been called a “Chinese Top”, which is a propeller on a stick. Of course it has no controllability, but has interesting aerodynamic properties including differential lift stabilization that will become important later in this paper.

In this work we explore a minimalistic device composed of just two rotors (or a rotor and a dragplate) with no swash plate, propelled by a single motor.

A simple flying toy called the Air Hogs Vectron Wave [21] has this structure. It flies in a stable manner, but is only controllable in the vertical direction. This device is passively stable. Understanding why it works and is stable is a central contribution of this paper.

In the next section we define the vehicle structure and its critical parameters, followed by the equations of motion describing the vehicle dynamics. Section IV presents an anal-

[1]Matthew Piccoli is a Ph.D. student of Mechanical Engineering and Applied Mechanics, University of Pennsylvania, Philadelphia, PA 19104, USA piccoli@seas.upenn.edu

[2]Mark Yim with the Department of Mechanical Engineering and Applied Mechanics, University of Pennsylvania, Philadelphia, PA 19104, USA yim@seas.upenn.edu

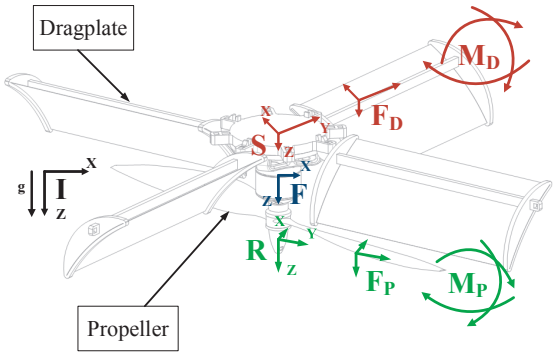

Fig. 1: Coordinate systems used while computing the equations of motion.

ysis of the passive stability of the vehicle and a model which can be used to understand the design parameters' effects on stability. The last sections verify the model, equations, and stability analysis with a variety of design implementations, which show both stability and instability.

II. PROPOSED VEHICLE

The device is minimalistic, composed of just two moving parts attached to a motor. A propeller is attached to the motor's rotor and a dragplate is attached to the motor's stator. There is no swash plate, no anti-torque tail rotor, and only one, instead of four, rotors. The main issue with the single propeller is controllability. Yim introduced a concept for attitude control of counter rotating propeller systems without a swashplate in [22] and, more recently, Paulos et al. [23] developed a simple hinged propeller that can induce control moments like a swashplate just by pulsing the propeller cyclically. This paper will not focus on this type of attitude control, though these methods are compatible with this device and are planned to be implemented after passive stability has been established.

The vehicle is illustrated in Figure 1 along with the frame assignments: S attached to the stator and R attached the rotor. The vehicle's single lifting propeller is mounted such that the thrust vector nominally goes through the center of mass (COM), lying on the Z axis of the collinear rotor and stator frames. Dragplates, which spin on the same axis, but in opposite direction from the propeller, are used to counter the propeller torque. Optionally, low Reynolds number airfoils are used on the dragplates to generate extra lift. The dragplates are arranged symmetrically around the propeller axis of rotation so the aerodynamic center of pressure (COP) also lies on the Z axis of the rotor or stator frames. Note that while COM and COP both lie on the z axis, they do not have to be designed to be coincident.

The signs of the velocities will become important in stability analysis. We will use Figure 1 as the example. Here the Z axis points downward. The rotor propeller spins with a right-handed positive rotation about Z. The dragplate are left-handed, rotating with a negative rotation about Z.

III. VEHICLE DYNAMICS

To control such a vehicle, we must understand its governing equations. It is a two body system: the stator and the rotor bodies. For the purposes of notation, aerodynamic forces and moments are felt by the dragplates, F_D, M_D, and the propeller, F_P, M_P, while frames are referenced to the stator and rotor, indicated by superscripted or subscripted S and R respectively. Additional frames, indicated with subscript and superscript I and F, are the inertial frame and the flyer frame. The flyer frame is a fictional frame at the COM whose Z axis has no rotational velocity relative to the environment (e.g. velocities of S and R relative F can yield aerodynamic properties), and can be thought of as the pilot's frame. Newton's equation is:

$$\dot{v}_F^I = (F_P + F_D + mg - m\omega^{FI} \times v_F^I)/m \tag{1}$$

where m is the mass of the whole vehicle. Euler's equation is:

$$\begin{aligned}\dot{\omega}^{FI} = (I_S^S + I_R^R + m^S\overline{S_{SF}}S_{SF} + m^R\overline{S_{RF}}S_{RF})^{-1} \\ (M_D + M_P - \omega^{FI} \times I_S^S\omega^{SI} - \omega^{FI} \times I_R^R\omega^{RI})\end{aligned} \tag{2}$$

where I_S^S the inertia of the stator in the stator frame, and S_{SF} is the skew-symmetric form of the displacement vector between the flyer frame and the stator frame. The rotor has its corresponding counterparts.

Position control of this vehicle is similar to that of a quadrotor, where in hover the thrust compensates exactly for gravity and the translational velocities depend on the attitude (roll and pitch) away from this nominal hover position.

IV. STABILITY

Part of controlling a vehicle involves stable motion. Unstable motion is characterized by unbounded velocities that ultimately lead to a crash. The active method of stability senses the state of the vehicle and controls velocities explicitly. A trivial passive method for imposing stability is to include large dampers such that any lateral motion is damped out. Forces eventually reach equilibrium at a terminal velocity. A more desirable stable condition is one in which unwanted velocities go to zero. In this type of vehicle we aim to passively orient its attitude, and thereby vector its thrust, in order to cancel any disturbance forces and reduce motion. This means that velocities in a given direction need rotations about the perpendicular axis.

Throughout this analysis, u, v, w, p, q, r will denote X, Y, Z linear and angular velocities in the flyer frame, ϕ, θ, ψ are the world to body euler angles, and X, Y, Z, L, M, N are the forces and moments in the flyer frame.

A. COP>COM

One type of stabilization can occur by introducing moments that cause a change in attitude, directing the thrust to slow translational velocities. Intuitively, as a vehicle with high dragplates (i.e. the COP has more negative z value than COM) translates through air, the air velocity pushes on the dragplates causing a moment about the COM which results in the downward thrust turning in the direction of translation

and slowing the vehicle down, passively stabilizing it. We will call this phenomenon COP>COM and was shown by Teoh et al. to stabilize the Robobee platform [24]

As an example, if a vehicle with this *COP>COM* feature is modeled as simple a rigid object in space and has only a velocity u, the *COP>COM* creates a moment, M, causing an angular acceleration which integrates to slow the X velocity.

$$\dot{\omega}^T = \begin{bmatrix} 0 & \frac{M}{I_{XY}} & 0 \end{bmatrix} \tag{3}$$

I_{XY} is the entire vehicle's inertia in the X and Y direction, which are treated as equal. This result is favorable for the Robobee which has no net angular momentum. Angular momentum will cause secondary reactions from gyroscopic effects. In the case of the proposed vehicle, integrating Equation (3) over time will result in nonzero ω_Y, which will yield a precession as seen from Equation (2), in this case an angular acceleration about the X axis.

$$\dot{\omega}^T = \begin{bmatrix} \frac{\omega_Y \omega_Z (I_{XY} - I_Z)}{I_{XY}} & \frac{M}{I_{XY}} & 0 \end{bmatrix} \tag{4}$$

Taking another step results in an added nutation in Y.

$$\dot{\omega}^T = \begin{bmatrix} \frac{\omega_Y \omega_Z (I_{XY} - I_Z)}{I_{XY}} & \frac{M + \omega_X \omega_Z (I_Z - I_{XY})}{I_{XY}} & 0 \end{bmatrix} \tag{5}$$

A number of values must be in the proper range for this method to stabilize a vehicle. In this case, with nonzero X velocity, stability requires a positive $\dot{\omega}_Y$. First, $M > 0$ must be true. This occurs when the COP is above the COM. Second, $M >> \omega_Y \omega_Z (I_{XY} - I_Z)$ to keep precession, and thus nutation, at a minimum.

B. Differential Lift

Another type of stabilization with restoring moments can be seen in the Chinese Top that passively orients its attitude using *differential lift*. This phenomenon applies moments to spinning propellers. As the device moves away from hover, with some linear velocity through the air, one side of the propeller sees a higher relative wind velocity, called the advancing side, and generates excess lift as a result. Conversely, the opposite, retreating side, generates less lift. This couple results in a moment about the direction of travel. Gyroscopic effects then result in an angular velocity perpendicular to this moment. The Chinese Top's attitude changes to slow the horizontal translation, passively stabilizing the vehicle.

For differential lift, the vehicle velocity in the positive X direction yields a negative moment, L, exclusively about the X axis as a result of the left-handed rotation of the dragplate:

$$\dot{\omega}^T = \begin{bmatrix} \frac{L}{I_{XY}} & 0 & 0 \end{bmatrix} \tag{6}$$

With one integration step we get the precession:

$$\dot{\omega}^T = \begin{bmatrix} \frac{L}{I_{XY}} & \frac{\omega_X \omega_Z (I_Z - I_{XY})}{I_{XY}} & 0 \end{bmatrix} \tag{7}$$

Another step yields the nutation:

$$\dot{\omega}^T = \begin{bmatrix} \frac{L + \omega_Y \omega_Z (I_{XY} - I_Z)}{I_{XY}} & \frac{\omega_X \omega_Z (I_Z - I_{XY})}{I_{XY}} & 0 \end{bmatrix} \tag{8}$$

For this method to stabilize the present vehicle with an initial X velocity, we again need a positive $\dot{\omega}_Y$. If the $I_Z > I_{XY}$ and the body with a higher angular momentum generates more differential lift, its corresponding precession will give a stabilizing torque. In the example of the vehicle in Figure 1, with dominant dragplates moving linearly in the positive X direction, ω_X is negative and ω_Z is a left-handed propeller and is thus also negative. Further, we want $\dot{\omega}_X$ to be relatively small compared to $\dot{\omega}_Y$. A large angular momentum in the Z direction allows for a large $\dot{\omega}_Y$. The nutation term will cancel the original undesired moment once the precession commences. If $I_{XY} > I_Z$, the sign of $\dot{\omega_Y}$ flips in Equation 7, requiring the body with less angular momentum to generate more differential lift to be stable. Again, this example assumes that there are no initial moments about the Y axis, i.e. the COP goes through the COM.

C. Design Implications

The math suggests two distinct designs. The first, *COP>COM*, case stabilizes itself when the net angular momentum is low and no net differential lift is produced. Larger angular momentum about Z increases the destabilizing effects from the precession and nutation from the *COP>COM* moments. Vehicles with an even number of symmetric contra-rotating propellers that in general cancel their rotational inertia, such as coaxial and quadrotors, fit this category, as well as propellerless vehicles like ornithopters. Unfortunately, multiple propellers implies multiple motors or complex transmissions, which adds complexity and cost.

The second case recommends a large angular momentum and large differential lift. In addition, it is better if the COP and COM are coincident in this case, since a large angular momentum coupled with a *COP>COM* will result in large destabilizing terms. To increase angular momentum, the dominating differential lift body should increase Z angular momentum. Because this is a flying vehicle, adding unnecessary weight to increase inertia is undesirable, thus the designer should aim to increase angular velocity.

One solution is more blades on the propeller. If the number of blades is indicated by B, then $I \propto B$, while $\omega \propto \sqrt{\frac{1}{B}}$, resulting in an increase in angular momentum, L, at the rate of $L \propto \sqrt{B}$. This assumes the increased mass is small compared to the entire vehicle, but if it were not, it would be expected that ω would be larger, and thus a more favorable angular momentum, to account for the extra thrust. Note that efficiency does decrease slightly by adding more blades.

$$\begin{bmatrix} \dot{u} \\ \dot{v} \\ \dot{p} \\ \dot{q} \\ \dot{\phi} \\ \dot{\theta} \end{bmatrix} = \begin{bmatrix} X_u & X_v & X_p & X_q & 0 & -g \\ Y_u & Y_v & Y_p & Y_q & g & 0 \\ L_u & L_v & L_p & L_q & 0 & 0 \\ M_u & M_v & M_p & M_q & 0 & 0 \\ 0 & 0 & 1 & 0 & 0 & 0 \\ 0 & 0 & 0 & 1 & 0 & 0 \end{bmatrix} \begin{bmatrix} u \\ v \\ p \\ q \\ \phi \\ \theta \end{bmatrix} \tag{9}$$

D. Stability Analysis

Proof of the vehicle's stability can be achieved with the Routh-Hurwitz criteria, which uses the linearized state transition matrix A in the form $\dot{x} = Ax$. This criterion depends on the characteristic equation $\det(A - \lambda I) = 0$,

which for a second order system is a polynomial of the form $a_2\lambda^2 + a_1\lambda^1 + a_0 = 0$, and states that stability is assured if and only if all $a_i > 0$, among other constraints for higher order polynomials. Linearization is done about hover.

Considering only the velocity and attitude terms in the state vector and ignoring rotations and translations in the Z direction, the state vector of the vehicle can be reduced from 18 to 6 terms: $\begin{bmatrix} u & v & p & q & \phi & \theta \end{bmatrix}^T$. To simplify notation, the linearized partial derivatives are rewritten as the force caused by the subscripted velocity normalized by mass or inertia, for example, $\frac{\partial X}{m\partial u} = X_u$ and $\frac{\partial L}{I_{XY}\partial p} = L_p$. The linearized equations of motion become Equation (9).

The linear forces perpendicular to the linear motion, X_v and Y_u, are very small in this configuration and these speeds, so we will ignore them. Similarly, linear drag caused by rotating the flyer is sufficiently small, so we can ignore X_p, X_q, Y_p, and Y_q as well.

In the linearized model about the hover condition, the state vector can be further reduced to $\begin{bmatrix} p & q \end{bmatrix}$, the roll rate and the pitch rate, since ϕ and θ are the integrals of p and q when using the small angle approximation. Variables u and v are functions of the integrals of ϕ and θ respectively. Symmetry around the vertical axis allows the combination of the remaining partial derivatives from the Jacobian. For convenience we rename the derivatives and describe them:

- $a = X_u = Y_v$
  is the drag force $\parallel$ to v and is always negative
- $b = L_u = M_v$
  is the differential lift moment $\parallel$ to v
- $c = L_v = -M_u$
  is the *COP>COM* moment $\perp$ to v
- $d = L_p = M_q$
  is the drag moment $\parallel$ to ω and is always negative
- $e = L_q = -M_p$
  is the gyroscopic precession $\perp$ to ω

After taking the Laplace transform, the resulting equation is:

$$\begin{bmatrix} sp \\ sq \end{bmatrix} = \begin{bmatrix} c\frac{g}{s(s-a)} + d & b\frac{g}{s(a-s)} + e \\ b\frac{g}{s(s-a)} - e & -c\frac{g}{s(a-s)} + d \end{bmatrix} \begin{bmatrix} p \\ q \end{bmatrix} \qquad (10)$$

The determinant of Equation (10) is:

$$\begin{aligned} 0 =& s^6 - 2(a+d)s^5 + (a^2 + 4ad + d^2 + e^2)s^4 \\ & - 2(a^2d + ad^2 + ae^2 + cg)s^3 \\ & + a^2(d^2 + e^2) + 2g(ca + cd - be))s^2 \\ & + 2ag(be - cd)s + g^2(b^2 + c^2) \end{aligned}$$

Executing the Routh-Hurwitz criteria on the above determinant gives stability constraints on the partial derivatives. One trivial result from the a_5 term is that a and d summed is negative. These terms are simply drag, indicating that the drag forces and moments express themselves in the opposite direction from motion and are always negative.

Another simple result from the a_1 term is that $cd > be$, since we already know a is negative and g is positive. The first term calls for COP>COM, since a negative c is COP>COM and d is always negative. The second term is from differential lift and gyroscopic precession, and suggests they be of opposite sign, which occurs when one body dominates differential lift and angular momentum. This shows the balance of the COP>COM versus differential lift methods.

Another constraint from Routh-Hurwitz commands $cg > (3ad + a^2 + d^2)(a + d) + de^2$. The first term on the right side indicates that more drag increases stability. The second term states that if the angular momentum has a large magnitude, COP can be lowered. Both can be thought of as requiring damping. Further constraints are possible to find; however, their complexity increases greatly from the previous examples.

V. SIMULATION

To help find viable parameters for new configurations, a simulator was developed in MATLAB. This dynamic simulator used the equations of motion from section III, as well as the Rankine-Froude equation for rotor disk inflow, motor equations, and blade element theory. This simulator allows the examination of parameters such as dragplate size and location, stator and rotor inertias, and propeller type.

To test for stability, the vehicle initially is oriented in the hover condition with a 0.1 radians error in the X roll direction. If a vehicle's states stabilize over time, then that vehicle presents a candidate for experimental verification.

It was found that the simulator claimed the virtual vehicles would be more stable than their real counterparts. A new parameter, a rotor tilt angle, was added to account for manufacturing errors. It makes the hover thrust not go through the COM. While the average moments created by this angle cancel after one revolution of the stator, virtual configurations that were once stable are no longer. Errors between 0.035 radians and 0.087 radians correlated well with real results.

VI. EXPERIMENTAL HARDWARE

The simulator guided the design of two prototypes, a wide variant (Figure 2) and a tall variant (Figure 3), each with variable elements. Some of the variable elements, which are shown in Figure 4, include dragplates of different sizes, location, and number as well as mounting arms for propellers with varying inertial and lift properties.

In the tall version, the dragplates have no lift and only provide anti-torque, while having very low angular momentum. This allows the propeller's angular momentum to outweigh that of the dragplates. Furthermore, the propeller is the only source of differential lift. The dragplates were created from a laser cut ABS frame and covered in a polyester film. Nine dragplates were constructed with varying COP distance in 5mm increments along Z.

The wide version features mounting points for up to eight dragplates. Unlike in the tall version, these dragplates both provide lift and inertia, achieving $I_Z > I_{XY}$. Beams of varying dragplate mounting heights were constructed, again out of laser cut ABS, and increment every 5mm with a total of 14 positions. Three types of airfoils were mounted to these frames. One type is seen mounted on the vehicle in Figure 2 and another is visible on the top right of Figure 4.

Fig. 2: Wide variant

Fig. 3: Tall variant

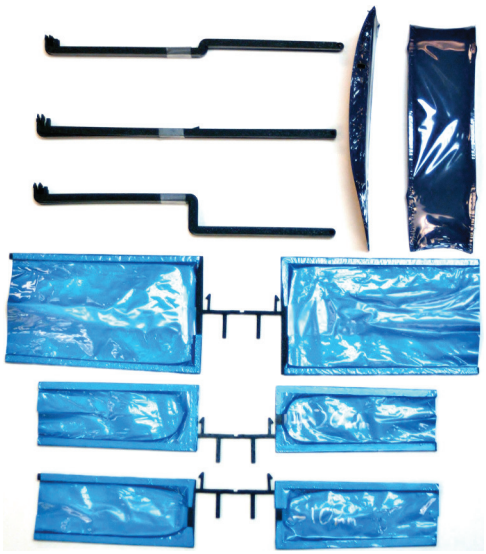

Fig. 4: Variable replaceable elements

A base housing the electronics and motor was created. A custom motor driver communicates to a computer running MATLAB over an AT86RF radio. The STM32F373 microcontroller commutes the E-Flight Park 400 740Kv brushless motor using an AS5145B encoder, records IMU data from an MPU-6050, and transmits data back to the computer. This base was mounted to both the tall and wide versions, and can be seen in both Figures 2 and 3.

VII. EXPERIMENTS AND RESULTS

Throughout the test, three parameters were varied. The most obvious is the height of COP vs COM by use of the interchangeable dragplates. Another is by varying the inertia through interchanging propellers and adding mass at the ends of the dragplates. Inertia is again varied by changing from the tall to wide version, switching I_{XY} to I_Z as the larger direction of inertia. Finally, the number of dragplate blades is varied to confirm that differential lift is the stabilizing moment and increases with the number of blades.

The results of a subset of trials is shown in Table I. Versions marked with a U in the Stable column were unstable. Those marked with U* were unstable, but remained aloft for more than 5 seconds before reaching a critical angle. The lone S is the stable vehicle and is the one shown in Figure 2. The I_Z refers to the rotor or stator I_Z, which ever is dominant (i.e. rotor I_Z for all of the tall configurations and stator for all wide configurations).

Despite having more configurations, the tall variant was always unstable. This agrees with the conclusions in Section IV-B that when $I_{XY} > I_Z$ the net differential lift must be generated by the body with less angular momentum. Since the dragplates were designed with a $\pi/2$ radian angle of attack, they create no lift, and thus no differential lift. Dragplates with angles of attack other than $\pi/2$ have been tested and show promise, but the vehicle was destroyed in a crash from instability. Footage is on the accompanying video.

The wide version was designed to generate lift from its dragplates. Initial versions utilized large Reynolds number airfoils at various angles of attack. Despite their position, shape, and size, no set had larger differential lift than the propeller's, which was in the opposite direction. Finally, a version that spanned the width of the crossbar was created, flown, and showed promise. The body of the version with four dragplates spun faster than the onboard IMU's limit of 34.9 $\frac{rad}{s}$, and therefore the listed angular momentum is <-0.02. This version precessed in the same direction despite large changes in COP>COM, which is an indication that the differential lift was insufficient, thus more blades were added. With eight blades, and small tweaking of the COM, the vehicle flew stably.

The COP to COM column in Table I lists the separation distance along Z, where negative values have COP above COM (the COP>COM condition). COM location is estimated from a 3D model and COP location is estimated as the centroid of the projected area on a vertical plane.

Note that the wide configurations all have positive COP to COM which is destabilizing to both *COP>COM* and differential lift mechanisms. It is likely that the centroid method of COP estimation likely indicates COP lower than it should be. This is because the thin bar and hoop structures on the wide configuration will have little aerodynamic effect and minimal pressure difference, yet will present a projected area that is significantly far from the estimated COP erroneously increasing their effect. Furthermore, shape and speed alter the drag significantly, and could be why the second to last configuration in Table I had a more favorable COP>COM

Ver	I_{XY}	I_Z	L	blades	to_{COM}^{COP}	Stable
	kgm^2	kgm^2	$\frac{rad}{s}$	$\#$	mm	
tall	3.3E-4	9E-5	-0.03	2	12	U
tall	3.3E-4	9E-5	-0.03	2	1.4	U
tall	3.3E-4	9E-5	-0.03	2	-1.2	U
tall	3.3E-4	9E-5	-0.03	2	-6.4	U
tall	3.3E-4	9E-5	-0.03	2	-9.0	U*
tall	3.3E-4	9E-5	-0.03	2	-15	U
tall	5.2E-4	2.1E-4	0.13	2	-8.4	U
tall	5.2E-4	2.1E-4	0.13	2	-3.1	U*
tall	5.2E-4	2.1E-4	0.13	2	2.0	U*
tall	5.2E-4	2.1E-4	0.13	2	9.9	U*
wide	1.2E-3	3.5E-3	<-0.02	4	12	U
wide	2E-3	3.5E-3	-0.04	8	8.2	U*
wide	2.6E-3	4.8E-3	-0.06	8	8.7	U*
wide	2.6E-3	4.8E-3	-0.06	8	10.3	S

* These unstable versions were stable for short periods (seconds)

TABLE I: Stability results of various vehicle configurations

than the last, stable configuration. The difference between the two configurations was the vertical location of the outer ring, visible in Figure 2. The unstable version had it at the bottom, while the stable configuration was with it as depicted. The ring may have generated more drag in the unstable configuration (while in the downwash of the propeller) or the dragplates may create more drag than estimated. Regardless, this measurement indicates that the COP did move, and certain locations were more stable than others.

VIII. CONCLUSION

We have explored a variety of flying configurations for a novel, simple, low cost flyer based on a single motor. We have identified two mechanisms for passive stability of flying devices we call *COP>COM* and differential lift, and discovered that they end up emphasizing conflicting design parameters. A large distance between COP and COM, required for *COP>COM* will destabilize the differential lift method. A large net angular momentum required for differential lift will destabilize *COP>COM*.

After fourteen trials of varying COP position, dragplate size, rotational inertia, and rotational speeds, one set of parameters was found to be stable. This successful design has been reduced to two optimizations. The first is minimizing the COP>COM effect by minimizing the distance between COP and COM. The second is maximizing the precession from differential lift by increasing the dominant body's inertia, and increasing the number of lifting blades.

There should be other parameters in the design space that also passively stabilize. The *COP>COM* method would work for a vehicle with similar angular momentum between rotor and stator and a large distance between COP and COM. This is left for future work. In the near future, combining the passive stability with control methods for arbitrary positioning by pulsing the one motor will be implemented.

REFERENCES

[1] S. Bortoff, "The university of toronto rc helicopter: a test bed for nonlinear control," in *Control Applications, 1999. Proceedings of the 1999 IEEE International Conference on*, vol. 1. IEEE, 1999, pp. 333–338.

[2] M. Matsuoka, A. Chen, S. Singh, A. Coates, A. Ng, and S. Thrun, "Autonomous helicopter tracking and localization using a self-surveying camera array," *The International Journal of Robotics Research*, vol. 26, no. 2, p. 205, 2007.

[3] J. Roberts, P. Corke, and G. Buskey, "Low-cost flight control system for a small autonomous helicopter," in *Australasian Conf. on Robotics and Automation*. Citeseer, 2002.

[4] E. Sanchez, H. Becerra, and C. Velez, "Combining fuzzy, pid and regulation control for an autonomous mini-helicopter," *Information Sciences*, vol. 177, no. 10, pp. 1999–2022, 2007.

[5] J. Morris, M. Van Nieuwstadt, and P. Bendotti, "Identification and control of a model helicopter in hover," in *American Control Conference, 1994*, vol. 2. IEEE, 1994, pp. 1238–1242.

[6] K. Sprague, V. Gavrilets, D. Dugail, B. Mettler, E. Feron, and I. Martinos, "Design and applications of an avionics system for a miniature acrobatic helicopter," in *Digital Avionics Systems, 2001. DASC. The 20th Conference*, vol. 1. IEEE, 2001, pp. 3C5–1.

[7] V. Gavrilets, E. Frazzoli, B. Mettler, M. Piedmonte, and E. Feron, "Aggressive maneuvering of small autonomous helicopters: A human-centered approach," *The International Journal of Robotics Research*, vol. 20, no. 10, p. 795, 2001.

[8] V. Gavrilets, B. Mettler, and E. Feron, "Dynamic model for a miniature aerobatic helicopter," in *AIAA Guidance Navigation and Control Conference, Montreal, Canada*, 2001.

[9] P. Samuel, J. Sirohi, F. Bohorquez, and R. Couch, "Design and testing of a rotary wing mav with an active structure for stability and control," in *Annual Forum Proceedings-American Helicopter Society*, vol. 61, no. 2. American Helicopter Society, Inc, 2005, p. 1946.

[10] D. Schafroth, S. Bouabdallah, C. Bermes, and R. Siegwart, "From the test benches to the first prototype of the mufly micro helicopter," *Unmanned Aircraft Systems*, pp. 245–260, 2009.

[11] Proxflyer, "Picoflyer description," http://www.avinc.com/nano, May 2011.

[12] N. Michael, D. Mellinger, Q. Lindsey, and V. Kumar, "The grasp multiple micro-uav testbed," *Robotics & Automation Magazine, IEEE*, vol. 17, no. 3, pp. 56–65, 2010.

[13] O. Purwin and R. D'Andrea, "Performing aggressive maneuvers using iterative learning control," in *Robotics and Automation, 2009. ICRA'09. IEEE International Conference on*. IEEE, 2009, pp. 1731–1736.

[14] G. Hoffmann, D. Rajnarayan, S. Waslander, D. Dostal, J. Jang, and C. Tomlin, "The stanford testbed of autonomous rotorcraft for multi agent control (starmac)," in *Digital Avionics Systems Conference, 2004. DASC 04. The 23rd*, vol. 2, oct. 2004, pp. 12.E.4 – 121–10 Vol.2.

[15] N. Michael, J. Fink, and V. Kumar, "Cooperative manipulation and transportation with aerial robots," *Autonomous Robots*, pp. 1–14, 2011.

[16] S. Bouabdallah, P. Murrieri, and R. Siegwart, "Design and control of an indoor micro quadrotor," in *Robotics and Automation, 2004. Proceedings. ICRA '04. 2004 IEEE International Conference on*, vol. 5, april-1 may 2004, pp. 4393 – 4398 Vol.5.

[17] S. Bouabdallah, A. Noth, and R. Siegwart, "Pid vs lq control techniques applied to an indoor micro quadrotor," in *Intelligent Robots and Systems, 2004.(IROS 2004). Proceedings. 2004 IEEE/RSJ International Conference on*, vol. 3. IEEE, 2004, pp. 2451–2456.

[18] G. Hoffmann, H. Huang, S. Waslander, and C. Tomlin, "Quadrotor helicopter flight dynamics and control: Theory and experiment," in *Proceedings of the AIAA Guidance, Navigation, and Control Conference*. Citeseer, 2007, pp. 1–20.

[19] P. Pounds, R. Mahony, J. Gresham, P. Corke, and J. Roberts, "Towards dynamically-favourable quad-rotor aerial robots," in *Australian Conference on Robotics and Automation*. Citeseer, 2004, p. 10.

[20] I. Kroo and P. Kunz, "Development of the mesicopter: A miniature autonomous rotorcraft," in *American Helicopter Society Vertical Lift Aircraft Design Conference*. American Helicopter Society, International (AHS), January 2000.

[21] G. Richards, "Christmas under control [toy industry]," *Engineering & Technology*, vol. 5, no. 18, pp. 42–43, 2010.

[22] M. H. Yim, "Tracking device," Patent US 6 422 509, 07 23, 2002.

[23] J. Paulos and M. Yim, "An underactuated propeller for attitude control in micro air vehicles,," in *Intelligent Robots and Systems (IROS), 2013 IEEE/RSJ International Conference on*. IEEE, 2013.

[24] Z. E. Teoh, S. B. Fuller, P. Chirarattananon, N. Prez-Arancibia, J. D. Greenberg, and R. J. Wood, "A hovering flapping-wing microrobot with altitude control and passive upright stability," in *Intelligent Robots and Systems (IROS), 2012 IEEE/RSJ International Conference on*. IEEE, 2012, pp. 3209–3216.